Accepted Manuscript

Mössbauer study of magnetism in Fe_3Se_4

R. Pohjonen, O. Mustonen, M. Karppinen, J. Lindén

PII: S0925-8388(18)30746-1

DOI: 10.1016/j.jallcom.2018.02.257

Reference: JALCOM 45133

To appear in: *Journal of Alloys and Compounds*

Received Date: 3 August 2017

Revised Date: 14 February 2018

Accepted Date: 20 February 2018

Please cite this article as: R. Pohjonen, O. Mustonen, M. Karppinen, J. Lindén, Mössbauer study of magnetism in Fe_3Se_4, *Journal of Alloys and Compounds* (2018), doi: 10.1016/j.jallcom.2018.02.257.

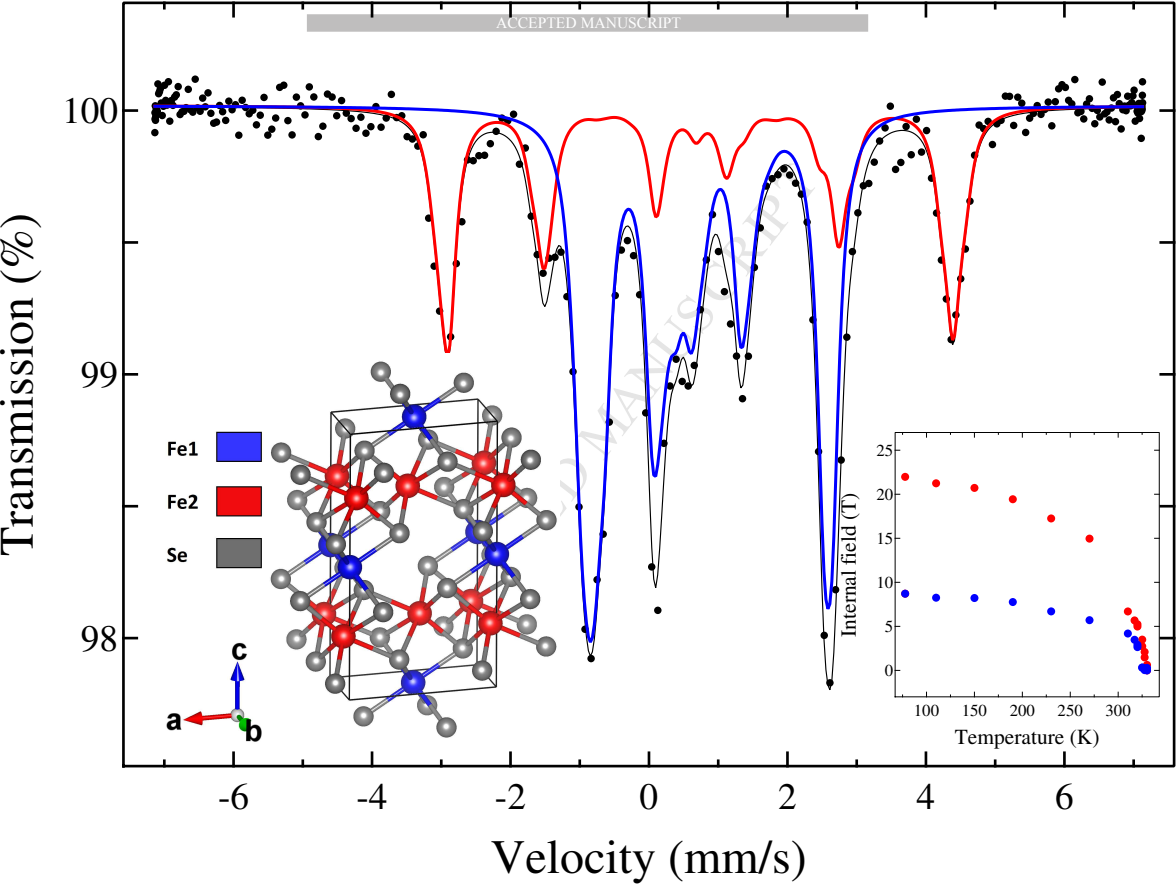

Mössbauer study of magnetism in Fe_3Se_4

R. Pohjonen[a], O. Mustonen[b], M. Karppinen[b], J. Lindén[a]

[a] *Åbo Akademi University, Faculty of Natural Sciences and Engineering/Physics, Porthansgatan 3, FI-20500 Turku Finland*
[b] *Aalto University, Department of Chemistry, Kemistintie 1, FI-00076 Aalto Finland*

Abstract

We have investigated the magnetism of ferrimagnetic Fe_3Se_4. A monoclinic Fe_3Se_4 powder sample was synthesized using an ampule technique. Magnetic properties were studied using ^{57}Fe Mössbauer spectroscopy measurements. The spectra were recorded between 77 and 360 K. Fitting could be done using four spectral components: two for each iron site in the lattice, or using only two components, each with a correlated distribution of the hyperfine parameters. Using the latter method the hyperfine parameter sets for each component were obtained from two distributions, tentatively taken as the local iron charge, i.e. the spectra were analyzed assuming the presence of a modulation of the iron valence. The crystallographic 1:2 ratio of the iron sites is reflected in the intensities of the magnetic Mössbauer spectra, whether one is using two or four components, but above T_C only the "correlated" two-component fitting was successful.

Key words: ^{57}Fe Mössbauer spectroscopy, iron selenide, fractional valence, ferrimagnetism

1. Introduction

The phase diagram of iron selenide is rather complicated with several structures existing only in very narrow compositional ranges [1]. The discovery of superconductivity in the paramagnetic β-FeSe [2] has renewed the interests in studying the Fe-Se system. There are also phases, which are magnetically ordered e.g. Fe_7Se_8[3] and Fe_3Se_4[4]. It is possible that there still are phases which have not been properly described yet. For example, in synthesis experiments of β-FeSe an unidentified paramagnetic secondary phase was observed [5].

Among the known Fe-Se phases monoclinic Fe_3Se_4 has several interesting properties. It has *e.g.* been suggested that Fe exhibits valence mixing similar to magnetite (Fe_3O_4) with an analogous charge balance of $Fe^{3+}Fe_2^{2.5+}Se_4^{2-}$, i.e. Fe at site 2 exhibits valence mixing[4, 6] The ratio between the populations at the two Fe sites is 1:2. There are, to our knowledge, rather few Mössbauer reports on bulk Fe_3Se_4. A layered Fe_3Se_4 sample with organic materials between the layers was recently studied using Mössbauer spectroscopy, but spectra are rather different from those obtained from bulk material.[7] Low-temperature ^{57}Fe Mössbauer spectra of bulk Fe_3Se_4 display two magnetic sextets with an intensity ratio of 1:2 reflecting the two iron lattice sites.[6] Slightly above room temperature Fe_3Se_4 undergoes a transition into an antiferromagnetically coupled structure, observed e.g. by neutron diffraction.[8, 9] However, as the spins do not cancel the overall phase is ferrimagnetic, with a Curie temperature (T_C) of 327 to 357 K, depending on the composition. The monoclinic structure does not change when the phase undergoes the magnetic transition.[4] The magnetic moments of the Fe atoms are comparatively low, judging by neutron diffraction[4, 10] data: $3.25\mu_B$ for site 1 and $1.94\mu_B$ for site 2. According to Ref. [10] the moments are along the [101] direction.

For the composition of the Fe_3Se_4 phase Okamoto reported a solid-solution range of 55.4-56.8 at.% Se[1] *i.e.*, the phase can be obtained only in a rather narrow compositional interval. In a more recent paper a slightly different range of 56.1-57.6 at.% is reported.[11] The phase has also been studied for a potential application as a hard magnetic material.[12, 13] The aim of this work is to study the properties of the magnetically ordered Fe atoms both above and below T_C using Mössbauer spectroscopy.

2. Experimental

For our investigation of a slightly non-stoichiometric Fe_3Se_4 compound we chose a selenium content of 56.1 at%. A synthetic $FeSe_{1.2779}$ sample was prepared by a solid-state reaction method. Appropriate quantities of powder Fe (99.99%) and ground shots of Se (99.99%) were mixed, pressed into a pellet at 10 kbar, sealed in an evacuated quartz tube, slowly heated up to 750 °C and annealed for 48 h. The resulting powder was reground, pressed into a pellet at 10 kbar, annealed again at 400 °C for 18 h and slowly cooled to room temperature. Powder X-ray diffraction data used for phase identification were collected at room temperature on a PanAnalytical X'Pert

Pro MPD diffractometer using Cu $K\alpha 1$ radiation. Rietveld analysis based on the monoclinic $I2/m$ (#12) space group for Fe_3Se_4 was used to confirm the origin of the observed peaks in the diffraction pattern.

The magnetic properties of the $FeSe_{1.2779}$ sample were characterized using ^{57}Fe Mössbauer spectroscopy in transmission geometry. The spectra were measured using a $^{57}Co : Rh$ source (Ritverc Co. 25 mCi sept. 2015) with a maximum Doppler velocity of 1.75-6.5 mm/s at temperatures between 77 and 360 K, where lower the velocities were used for following the demise of the magnetic hyperfine field. The sample was cooled using an Oxford CF506 continuous-flow cryostat with liquid N_2 as coolant. Temperatures above 330 K were reached using a home-built resisistive heater, flushed with a small stream of dry N_2 gas to prevent sample oxidization. The temperature was controlled using a Keithley 2510 TEC SourceMeter. Initially, all magnetic spectra were fitted using four Mössbauer components, each representing a specific Fe species in the lattice. Below T_C each component consists of a six-line spectrum analyzed using the following fit parameters: magnetic hyperfine field B acting on the Fe nucleus, electric quadrupole coupling constant eQV_{zz}, the so called asymmetry parameter η, the angle β between the direction of B and V_{zz}, the isomer shift δ relative to α-Fe, and relative component intensity I. The line width Γ was fitted but constrained equal for all lines and components. The electric quadrupole coupling constant, consists of the quadrupole moment eQ of the excited ^{57}Fe nucleus and the main component of the electric field gradient $V_{zz} \equiv \frac{\partial^2 V}{\partial z^2}$, where V is the electric potential. The unitless asymmetry parameter defined as

$$\eta = \frac{|V_{yy} - V_{xx}|}{|V_{zz}|} \tag{1}$$

measures the asymmetry of the electric field. In a second attempt the number of Mössbauer components were reduced to two. Instead, histogram distributions, effectively modulating the local iron valence were introduced for each component. A charge interval $q \in [0, 1]$ was divided into partitions q_i, with i running from 1 to 20. As the unit of the charge is arbitrary, the absolute width of the interval in charge units is not fixed. Each q_i was given a none-negative weight h_i taken as a fit parameter. The isomer shift and quadrupole coupling have a direct dependence on the iron charge, while the internal field depends indirectly upon it through the electron spin. Hence, when fitting eQV_{zz}, δ, and B the following generic expression was used for

each temperature-dependent hyperfine parameter:

$$p_i(T) = p_0(T) + \alpha(T)q_i, \tag{2}$$

where $p_0(T)$ is the value of the hyperfine parameter if the histogram is omitted, *i.e.* it gives the value for the hyperfine parameter in the absence of the valence modulation and $\alpha(T)$ scales the span of distribution. In this manner the distribution for all hyperfine parameters for a specific iron site depend on the same charge histogram. Two such histograms where used - one for each lattice site. Effectively each Mössbauer component consists of twenty sub-components with a statistical weight given by the relative height h_i of each partition q_i, with the additional requirement that $\sum_i h_i = 1$.

3. Results and discussion

3.1. X-ray diffraction

The X-ray diffraction pattern and the unit cell of the $FeSe_{1.2779}$ sample are displayed in Fig. 1. All observed peaks can be indexed with reflections of the monoclinic Fe_3Se_4 structure.[4, 11] Possible impurities are therefore below the detection limit. The fitted values for the lattice parameters were $a = 6.20238(3)$ Å, $b = 3.53183(2)$ Å, $c = 11.33099(6)$ Å, and $\beta = 91.8252(3)°$. Rietveld analysis gave a 1:2 ratio for the iron lattice sites 1 and 2.

3.2. Mössbauer spectra

The Mössbauer spectrum recorded at 110 K is displayed in Fig. 2. In the upper panel the fitting was done using four sextets and in the lower using only two, but with distributions for the hyperfine parameters. Using only two simple sextets with no distributions yielded poor fittings and was therefore immediately abandoned. In the four-component fitting one of the two low-field components exhibited excessive broadening, which is curious as it should originate from the same iron site as the other low-field component, which did not exhibit broadening. This effect disappeared when the number of components was reduced to two and hyperfine parameter distributions were released. Furthermore, the experimental line width Γ remained close to the "thin-absorber limit" around 0.25 mm/s, or slightly below, except around T_C where the spectra were slightly broadened and Γ reached 0.30 mm/s. In the paramagnetic regime Γ returned to $\sim$ 0.25 mm/s. Throughout the temperature range the intensity ratio for the two components remained close to 2:1, Fig. 3. Only around T_C some deviations occurred.

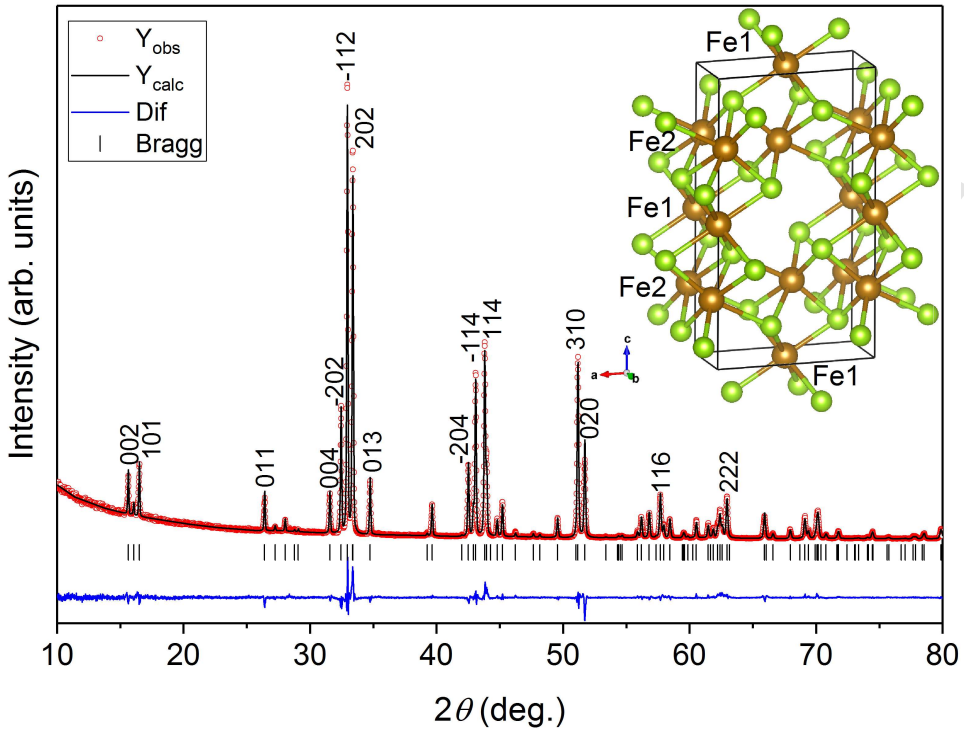

Figure 1: Fitted X-ray diffraction pattern for $FeSe_{1.2779}$. Ticks denote the positions of the identified peaks and the difference between fitting and data is displayed below the ticks. Main reflections are indexed up to $2\theta \approx 65°$. Inset: The unit cell of Fe_3Se_4, with Fe atoms in brown(dark gray) and Se in green (light gray).

Independent of the fitting scheme the average internal magnetic fields are too low for regular high-spin Fe^{3+} or Fe^{2+} with $B \approx 23$ T for site 1 and $B \approx 8$ T for site 2, Fig. 4. Typical saturation values are ~ 53 T for Fe^{3+} and ~ 42 T for Fe^{2+}, as trivalent iron has five majority-spin electrons and the divalent one additionally one minority-spin electron. Such fields correspond to iron magnetic moments of $\sim 5\mu_B$ and $\sim 4\mu_B$, respectively. The average valence of Fe, assuming Se^{2-} is +2.67, which would bring the internal field slightly down from the high-spin trivalent value. The coordination octahedron around site 1 is rather regular and hence the crystal-field splitting ought to be moderate, while the coordination octahedron around site 2 is much more deformed and this could give rise to substantial crystal-field splitting, which could cause Fe to reside in an intermediate-spin state. As the fields

are low most probably both Fe species are in the intermediate spin-state, in which case also dipolar and orbital contributions could be present, further counteracting the regular spin contribution. A dipolar contribution arises if the co-occupancy of the minority and majority-spin electron is confined to a particular *d*-orbital, instead of being distributed on several orbitals. This would then bring down the internal field considerably as a dipolar contribution can be several tens of Tesla.[15] As Fe_3Se_4 is probably more covalent than ionic it is hard to make reliable estimates of the contributions to the internal field, even the spin-only contribution mediated by the Fermi-contact interaction may vary. As high-spin Fe^{3+} has a magnetic moment of 5 μ_B the intermediate-spin magnetic moment is 3 μ_B, but when the formal valence is +2.67 the intermediate magnetic moment and corresponding internal field could be roughly 3.67 μ_B & 38.9 T or 2.33 μ_B & 24.7 T, depending on how the fractional valence affects the moment. Interestingly the ratio of these two extremes are roughly the same as that obtained from neutron scattering: 3.25:1.94 for the two Fe sites. Dipolar contributions cannot be observed by neutron scattering, but if we surmise that the above two estimates for the magnetic moments corresponds to the two Fe sites, then a antiparallel dipolar field of $\sim$ 12 T or $\sim$ 16 T is acting on Fe nuclei, depending if the neutron-scattering values or the estimated values are used. These are not inconceivably large for a dipolar field caused by a non-spherical, i.e. an intermediate-spin configuration.

The 77-K isomer shift values (Fig. 7) of 0.78 mm/s for site 1 and 0.70 mm/s for site 2 are both slightly shifted towards divalency, in particular the former. Both values are compatible with the intermediate spin state, shifted slightly towards divalency due to the fractional valence state.[14]

While the magnetic fields are rather low, the experimental quadrupole coupling constants (Fig. 8) are rather substantial, i.e. the influence of both the electric and magnetic hyperfine interactions were of similar order. Therefore, the angle β and the asymmetry parameter η could be released in the fittings. Generally β was very close to $-90°$ for Fe at site 1 and $+90°$ for site 2. Point-charge calculations for the selenium ions contribution to the electric field gradient acting on the Fe nuclei gave rather modest values for V_{zz}, indicating that there must be a substantial valence electron contribution, no doubt caused by the intermediate-spin configuration, because a substantial dipolar contribution is also connected to a large valence-electron contribution to the electric field gradient.[15]

Non-zero η values are to be expected for a monoclinic structure, but

generally η is notoriously hard to fit reliably. Except around T_C η remained close to 0.6 for site 1 and 0.4 for site 2, *i.e.* it was surprisingly stable.

The histograms for the magnetic fields obtained from the fittings are displayed in Figs. 5 and 6. For the quadrupole coupling constant and the isomer shift the histograms are almost identical to the magnetic one, except that the span and midpoint of the x-axis is different, in accord with eq. 2. They also reach to temperatures beyond T_C, whereas for the magnetic field $p_0(T_C) = \alpha(T_C) = 0$, *i.e.* the internal fields are zero above T_C. The Curie temperature interpolated from the field data is 331 K, Fig. 4. For both sites the histogram of the magnetic field is peaked around two separate field values, explaining why the four-component fitting was also successful. Such double peaks can be taken as a sign that there is a two-peaked distribution of the valence within the iron site.

Average hyperfine parameters for each iron site are readily obtained by "integrating" eq. 2:

$$\langle p_i(T) \rangle = p_0(T) + \alpha(T) \sum_{i=1}^{20} h_i q_i. \tag{3}$$

The hyperfine parameters plotted as a function of temperature, in Figs. 4,7, and 8 were obtained by applying Eq. 3 to the histogram data. Interestingly, the histograms are needed also above T_C, as it is impossible to fit the data using only two paramagnetic doublets due to the two sites. In this region our four component fitting failed, as it was not possible to find a combination retaining the 1:2 intensity ratio by grouping the components in two pairs. However, the histogram distributions become narrower at T_C and practically point-like for site 2, while site 1 still exhibits a substantial spread. A paramagnetic spectrum recorded at 360 K, is displayed in Fig. 9 and the spreading of component 1 is evident.

In the region just below T_C the fitting becomes increasingly difficult, as the fluctuating atomic spins causes the internal field distributions to blur. Thus the sudden drop for the quadrupole coupling constant of Fe at site 1 may be a simple artifact of fitting, Fig. 8, but the cross over seems to be a real effect. The isomer shifts, Fig. 7 exhibit a more monotonic decrease, typically caused by the temperature-dependent second-order Doppler shift.[16] Above T_C the isomer shifts of the two components converge, which may indicate that the paramagnetic moments of site 1 and 2 converge. Above T_C the isomer shift values have crossed like the quadrupole coupling constants, which could

indicate a slight charge transfer between the iron sites, enabled due to the disappearance of the antiferromagnetic coupling between the two Fe sites.

4. Conclusions

A non-stoichiometric monoclinic Fe_3Se_4 sample was successfully synthesized and studied by ^{57}Fe Mössbauer spectroscopy at various temperatures. The two iron sites were readily identified from the two magnetic sextets observed below $T_C \approx 331$ K. Both sextets exhibits sign of broadening, which could be dealt with either by doubling the number of sextets to four or by introducing a correlated histogram distribution to each sextet. It is inferred that the origin of the distribution is a charge-distribution occurring within each iron site. At T_C the distribution narrows down, but remains still considerable for iron at lattice site 1 up to at least 360 K - the highest temperature reached in this work.

The internal fields for the iron atoms are low. For both sites the average field is considerably below the expected high-spin values, which is interpreted as a intermediate-spin state, with additional antiparallel contributions from the dipolar field of the doubly-occupied *d* orbital, which is in accord with the large quadrupole coupling constant observed.

References

[1] H. Okamoto, in:"Phase Diagrams of Binary Iron Alloys". H. Okamoto (ed.), Materials Information Soc., Materials Park, Ohio (1993).

[2] F.-Ch. Hsu, J.-Y. Luo, K.-W. Yeh, T.-K. Chen, T.-W. Huang, Ph. M. Wu, Y.-Ch. Lee, Y.-L. Huang, Y.-Y. Chu, D.-Ch. Yan, and M.-K. Wu, Proc. Natl. Acad. Sci. U.S.A. 105 (2008) 14262.

[3] C. Boumford, A.H Morrish, Physica Status Solidi (A) 22 (1974) 435.

[4] B. Lambert-Andron and G. Berdias, Solid State Communications, 7 (1969) 623-629.

[5] A. Sklyarova, J. Lindén, G.C. Tewari, E.-L. Rautama, and M. Karppinen, Hyp. Int. 226 (2014) 341-349.

[6] J.R. Régnard and J.C. Hocquenghem, J. Phys. Colloques, 32 (1971) C1-268-270.

[7] C. Pak, S. Kamali, J. Pham, K. Lee, Joshua T. Greenfield, and K. Kovnir, J. Am. Chem. Soc., 135 (2013), 19111-19114.

[8] A.F. Andresen, Acta Chem. Scand. 22 (1968) 827-835.

[9] A.F. Andresen and B. van Laar, Acta Chem. Scand. 24 (1970) 2435-2439.

[10] B. Lambert-Andron, G. Berdias, and D. Babot, J. Phys. Chem. Solids 33 (1972) 87-94.

[11] S. Li, S.F. Lin, J. Ji, Z.N. Guo, and W.X. Yuan, Powder Diffraction 28 (2013) S32-S36.

[12] M.S. Bishwas, R. Das, and P. Poddar, The Journal of Physical Chemistry C, 118 (2014) 4016-4022.

[13] I.S. Lyubutin, Chun-Rong Lin, K.O. Funtov, T.V Dimitrieva, S.S. Starchikov, Yu-Jhan Siao, and Mei-Li Chen, The Journal of Chemical Physics, 141 (2014) 044704-10.

[14] N.N. Greenwood, T.C. Gibb, in *Mössbauer Spectroscopy, 1st ed.* (Chapman and Hall, London 1971) p. 93.

[15] J. Lindén, F. Lindroos, and P. Karen, J. Solid State Chem. 252 (2017) 119-128.

[16] N.N. Greenwood, T.C. Gibb, in *Mössbauer Spectroscopy, 1st ed.* (Chapman and Hall, London 1971) pp. 50-53.

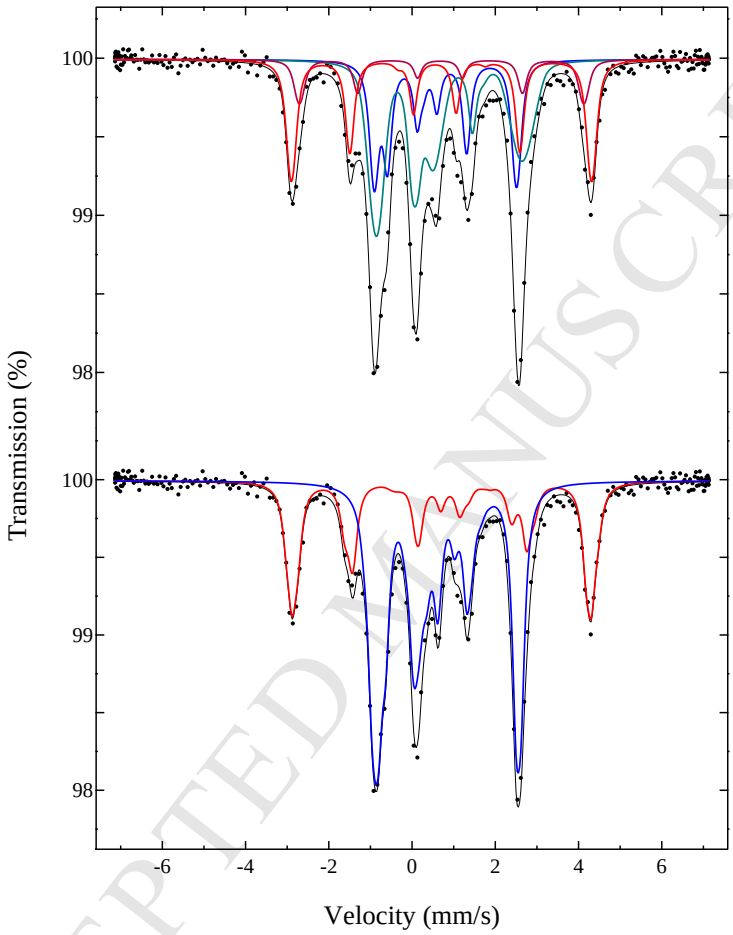

Figure 2: Mössbauer spectrum of the $FeSe_{1.2779}$ sample recorded at 110 K fitted using four components (upper panel) and two components with histogram distributions for the hyperfine parameters (lower panel), see text. The reddish (large internal field) components are assigned to Fe at site 1 and the bluish (low internal field) to Fe at site 2.

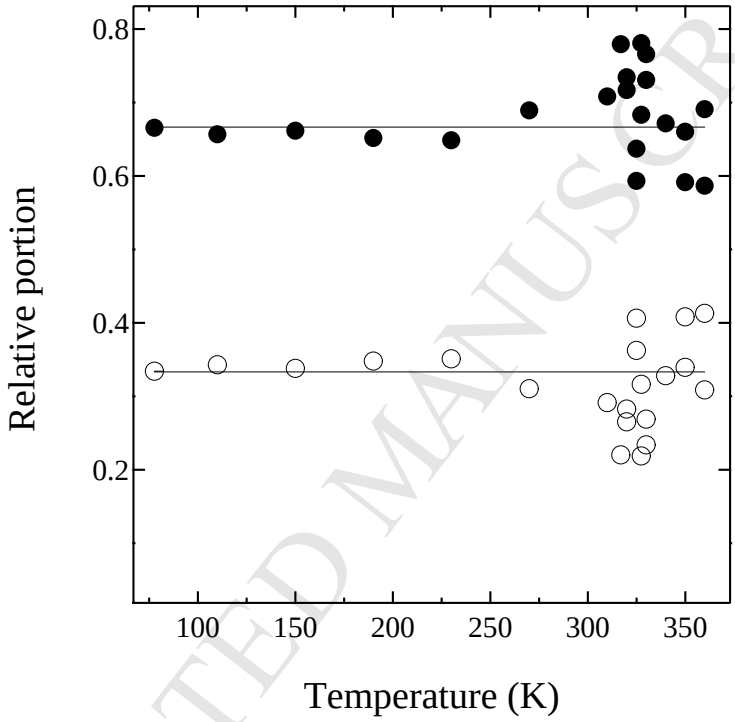

Figure 3: Relative intensities for the two components, originating from site 1 ∘ and site 2 •. Horizontal lines indicate the theoretical intensities corresponding to the multiplicity of the two sites.

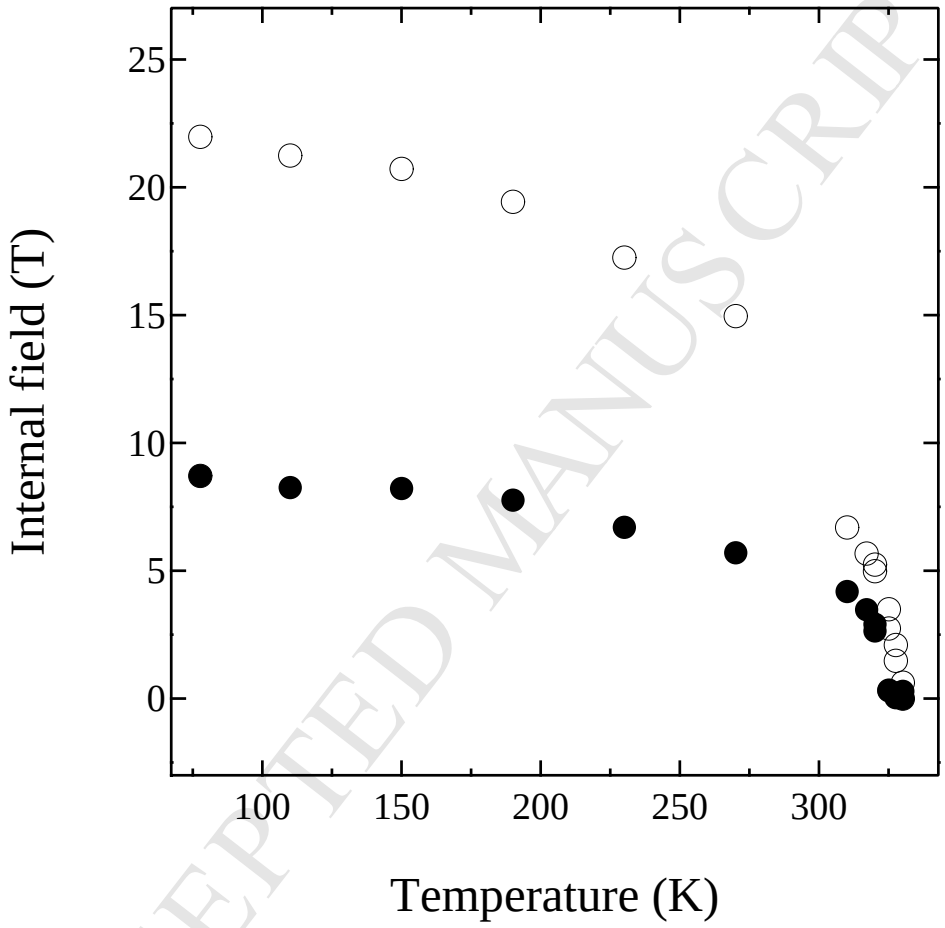

Figure 4: Average internal field for Fe at site 1 ∘ and site 2 •.

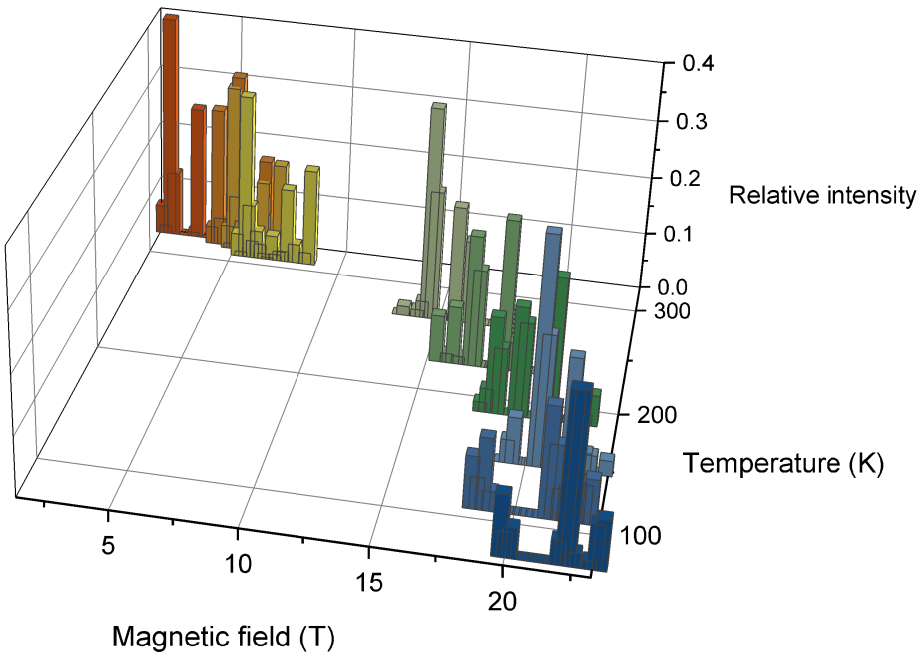

Figure 5: Histogram for internal magnetic field of Fe at site 1 vs. temperature. The histogram data was obtained by fitting the Mössbauer spectra, see text.

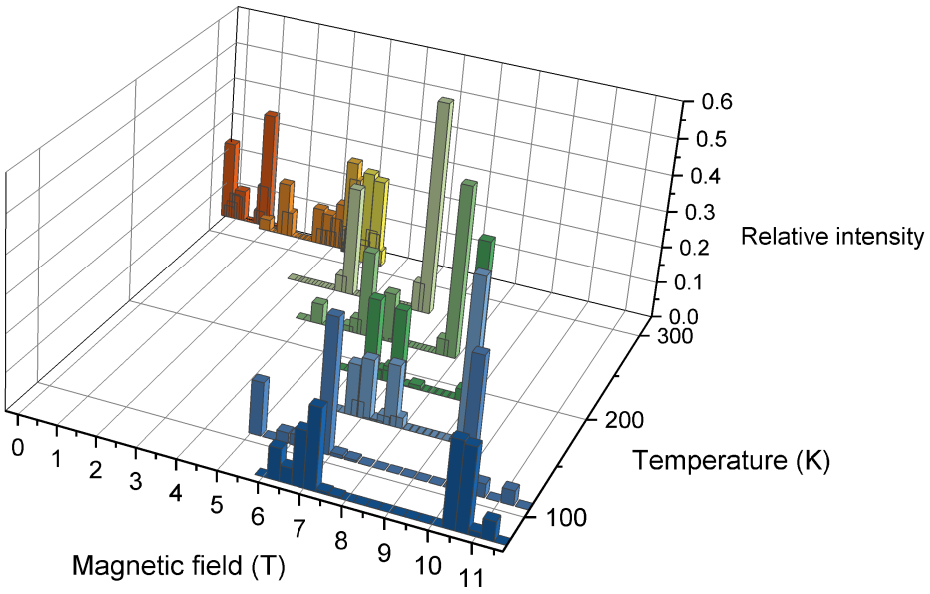

Figure 6: Histogram for internal magnetic field of Fe at site 2 vs. temperature. The histogram data was obtained by fitting the Mössbauer spectra, see text.

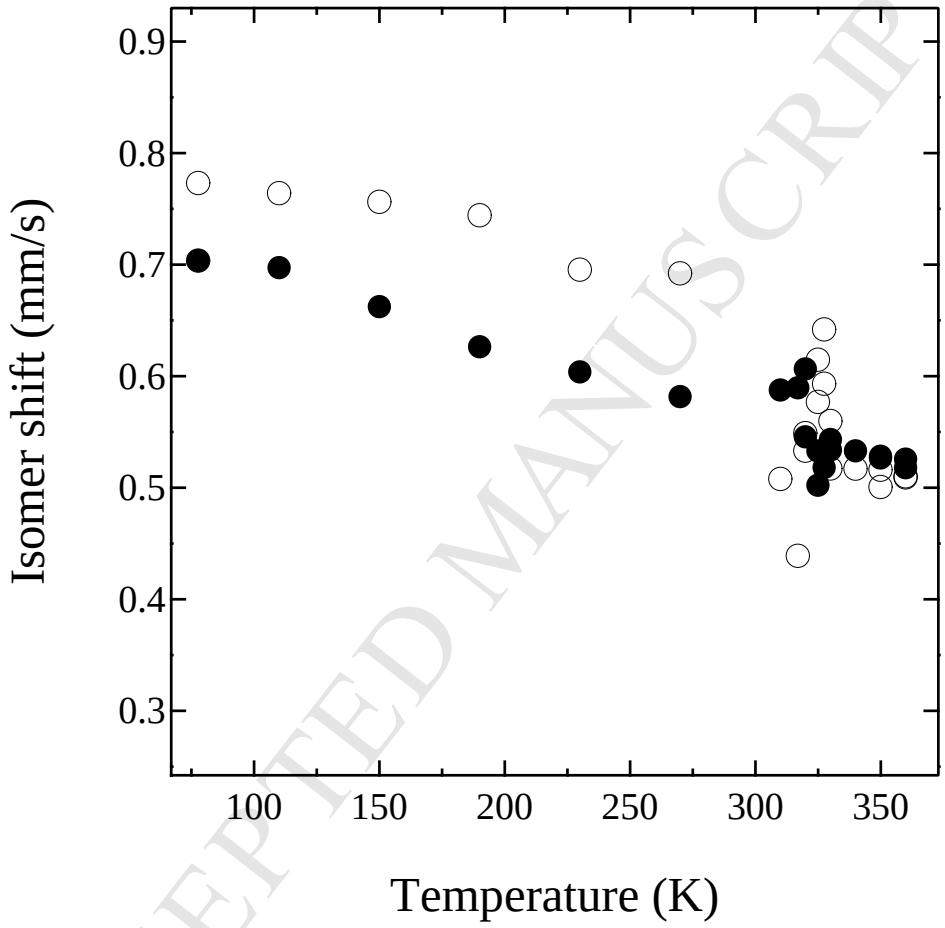

Figure 7: Average isomer shifts for Fe at site 1 ○ and site 2 ●.

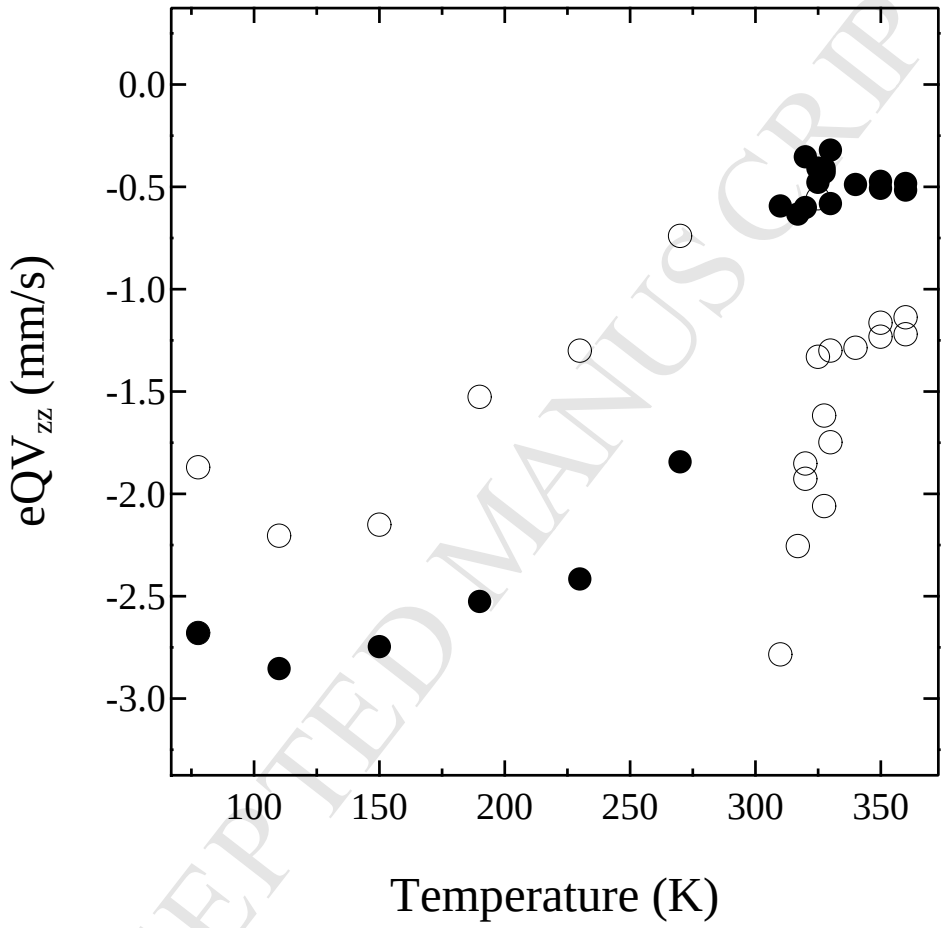

Figure 8: Average quadrupole coupling constants for Fe at site 1 ∘ and site 2 ●.

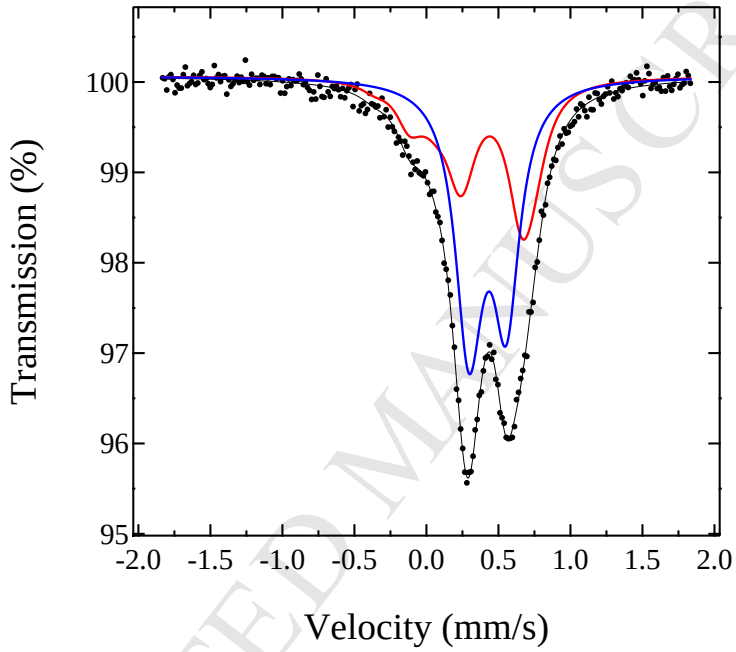

Figure 9: Mössbauer spectrum of the $FeSe_{1.2779}$ sample recorded at 360 K fitted using two components with histogram distributions for the hyperfine parameters, see text. The red (low intensity) component is assigned to Fe at site 1 and the blue (high intensity) to Fe at site 2.

- A high-purity monoclinic Fe_3Se_4 sample is successfully synthesized
- Evidence for partial valence-mixing in Fe_3Se_4 is found
- A histogram-based fitting for the complicated Mössbauer data is developed and successfully applied to the analysis of the spectra
- The origin of the rather low magnetic hyperfine fields in Fe_3Se_4 is discussed